ECAS 2016

sciforum

Conference Proceedings Paper

Sensitivity of the Reaction Mechanism for the Ozone Depletion Events during the Arctic Spring on the Initial Atmospheric Composition of the Troposphere

Le Cao *, Min He and Nianwen Cao

Published: 15 July 2016

Key Laboratory for Aerosol-Cloud-Precipitation of China Meteorological Administration, Nanjing University of Information Science and Technology, Nanjing 210044, China

* Correspondence: le.cao@nuist.edu.cn

Abstract: The ozone depletion events (ODEs) in the spring of Arctic has been investigated since the 1980s. It is found that the depletion of ozone is highly associated with the release of halogens especially bromine containing compounds from various substrates such as the ice/snow-covered surfaces in Arctic. In the present study, the dependence of the mixing ratios of ozone and principal bromine species during ODEs on the initial composition of the atmosphere in the boundary layer of Arctic is investigated by using a concentration sensitivity analysis, which is performed by implementing a reaction mechanism representing the ozone depletion and halogen release in a box model KINAL. The ratio between the relative change of the mixing ratios of particular species such as ozone and the variation in the initial concentration of each atmospheric component is calculated, which reveals the relative importance of each initial species in the chemical kinetic system. The simulation results show that the impacts of various chemical species are different for ozone and bromine containing compounds during the depletion of ozone. It is found the species CH_3CHO is the most influential species which critically controls the time scale of the complete removal of ozone. However, the rate of ozone depletion and the maximum values of bromine species are only slightly influenced by the presence of CH_3CHO. Besides, according to the concentration sensitivity analysis, the reduction of initial Br_2 is found to cause a significant retardant of the ODE while the initial mixing ratio of HBr exerts minor influence on both ozone and bromine species. In addition, it is also interesting to note that the increase of C_2H_2 would significantly raise the amount of HOBr and Br in the atmosphere while the ozone depletion is hardly changed.

Keywords: concentration sensitivity analysis; ozone depletion event; bromine explosion mechanism

1. Introduction

Due to its unique role in the lower atmosphere, ozone has become the focus of the scientific community since its first discovery by Dr. Schoebein in 1840 [1]. In the stratosphere, ozone is called "good ozone", as it is capable of absorbing most of the Ultra-Violet (UV) radiations from the Sun, thus protecting the lives on the earth. Moreover, ozone in the upper part of the stratosphere plays the role of converting the radiation to heat so that the top of the stratosphere is warmed. As a result, a temperature inversion is formed in the stratosphere, which leads to the existence of the layer. In contrast to that, in the troposphere, ozone is a kind of pollutant which has a mixing ratio of 20-60 ppb on average (ppb = parts per billion) [2]. It is found by Lippmann [3] that an exposure of healthy adults to a 100 ppb ozone environment for several hours would lead to a reduction of the lung function of these people. Furthermore, this harmful effect brought about by excessive amount

of the tropospheric ozone accumulates when the exposure time is extended. Apart from this, ozone in the troposphere also destroys living tissue, causes eye irritation and chest pain to individuals [4]. Therefore, the tropospheric ozone is also called "bad ozone". Since ozone in the troposphere originate from several precursors such as hydrocarbons and nitrogen oxides (NO_x) which are produced from human activities such as gasoline vapors, power plants of fossil fuel and automobile emissions, due to the growing population and industrial activities, tropospheric ozone mixing ratio has more than doubled since 1900 [5].

In the 1980s, an abnormal decline in the mixing ratio of the tropospheric ozone in polar regions was reported from various sites such as Barrow, Alaska [6] and Alert, Canada [7] during the springtime. In these observations, the surface ozone mixing ratio is found to drop from its background level ($\sim$40 ppb) to less than 1 ppb or even under the detection limit in a couple of days, which is then named as "ozone depletion events" (ODEs). Furthermore, a strong enhancement of halogen species especially bromine containing compounds in the troposphere during ODEs is also noticed [8]. A good agreement between the decline of ozone and the rise of bromine amount in the troposphere is found, which indicates the importance of bromine in the destruction of ozone. Later on, Hönninger and Platt [9] revealed that bromine monoxide (BrO) is involved in an auto-catalytic reaction cycle in which ozone is consumed without any loss of bromine. It is suggested by Hönninger and Platt [9] that BrO participates in the self-reactions,

$$\mathrm{BrO} + \mathrm{BrO} \rightarrow \mathrm{Br_2}\ (\text{or } 2\mathrm{Br}) + \mathrm{O_2}, \tag{R1}$$

in which Br_2 or Br atoms are formed. In the presence of sunlight, Br_2 is rapidly photolyzed and converted to Br which continues to destroy ozone in the troposphere as follows,

$$\mathrm{Br_2} + h\nu \rightarrow 2\mathrm{Br}, \tag{R2}$$

$$\mathrm{Br} + \mathrm{O_3} \rightarrow \mathrm{BrO} + \mathrm{O_2}. \tag{R3}$$

However, the reaction sequence (R1)-(R3) cannot explain the sharp increase of bromine during ODEs. Thus, apart from reactions (R1)-(R3), it is also suggested that the gas-phase hypobromous acid (HOBr) formed by the oxidation of BrO is able to activate bromide from various polar substrates such as the suspended aerosols and ice/snow-covered surfaces, leading to an explosively increase of the total bromine amount and also a rapid ozone depletion in the troposphere. This process can be expressed as

$$\begin{aligned}
\mathrm{Br} + \mathrm{O_3} &\rightarrow \mathrm{BrO} + \mathrm{O_2} \\
\mathrm{BrO} + \mathrm{HO_2} &\rightarrow \mathrm{HOBr} + \mathrm{O_2} \\
\mathrm{HOBr} + \mathrm{H^+} + \mathrm{Br^-} &\overset{\mathrm{mp}}{\rightarrow} \mathrm{Br_2} + \mathrm{H_2O} \\
\mathrm{Br_2} + h\nu &\rightarrow 2\mathrm{Br} \\
\hline
\text{Net}: \mathrm{O_3} + \mathrm{HO_2} + \mathrm{H^+} + \mathrm{Br^-} + h\nu &\overset{\mathrm{mp}}{\rightarrow} 2\,\mathrm{O_2} + \mathrm{Br} + \mathrm{H_2O}.
\end{aligned} \tag{R4}$$

In the reaction sequence (R4), "mp" represents multiphase reactions which occur in or on the suspended aerosols and the surfaces covered by ice and snow. It is seen from (R4) that through this reaction sequence, a bromide ion stored in the substrates is activated by HOBr, and consequently converted to Br which resides in the troposphere and consumes ozone. As a result, the total gas-phase bromine loading in the troposphere is exponentially raised, and this reaction sequence is named as "bromine explosion" mechanism [9–12].

The tropospheric ODEs and the associated bromine explosion phenomenon have a great influence on the lives on the earth and also the climate of polar regions. During ODEs, the oxidation ability of the atmosphere in the troposphere is dominated by the bromine containing compounds instead of ozone. As a result, more reactive gas mercury (RGM) are formed and then deposit on the

ground surface. In late spring or summertime, due to the increase of the temperature, the deposited RGM are carried by the melted snow, flowing into the ocean. Through the oceanic circulation, RGM would consequently enter the body of people at mid-latitudes, damaging their health. Furthermore, as ozone is also a type of greenhouse gas which warms the surface of polar regions, the decline of the ozone mixing ratio during springtime would modify the melting speed of glacier so that the climate of polar regions is influenced.

In order to investigate the physical and chemical processes related to ODEs, a large amount of studies have been performed previously. Generally, the occurrence and termination of ODEs are determined by the joint effect of the local chemistry, vertical turbulent mixing, and long-range transport. As discussed above, the major chemical pathways for the production and destruction of ozone during ODEs are the brominated reaction sequences (R1)-(R4) [10–12], and this bromine chemistry consists of gas-phase reactions as well as the heterogeneous reactions for releasing bromine to the ambient air. The importance of vertical mixing in the boundary layer was first indicated by Lehrer *et al.* [13] by using a one-dimensional model FACSIMILE. According to their simulation results, they proposed that when a temperature inversion is formed on the top of the boundary layer, the turbulent diffusivity above the boundary layer becomes smaller. Therefore, the ozone-rich air in the free troposphere is hardly to be mixed into the boundary layer by the turbulent diffusion, which favors the occurrence of ODEs in the boundary layer. Apart from these two mechanisms, ODEs are also influenced by the long-range transport of the air. Strong *et al.* [14] and Morin *et al.* [15] pointed out that the ODEs observed at Alert, Canada originate from the air which has contacted with the newly-formed fresh sea ice to the northwest of Alert. In contrast to that, when the ozone-rich air influenced by the inland multi-year sea ice is transported from the south to Alert, the low-ozone episodes in Alert are terminated. Their conclusions are also confirmed by the observations conducted by Jones *et al.* [16]. A thorough review of the existing studies on ODEs is given by Platt and Hönninger [10], Simpson *et al.* [11] and Abbatt *et al.* [12].

Recently, studies on the sensitivities of ozone and principal bromine containing compounds during ODEs on the amount of bromine in the initial atmospheric composition were performed [17]. Besides, the dependence of the ozone depletion rate on the prescribed fluxes of halogen species such as Br_2 and BrCl was also investigated by Evans *et al.* [18], and Piot and Von Glasow [19,20]. However, this kind of sensitivity study is normally performed in a "brute force" way in which the initial mixing ratio of each component of the atmosphere is varied by a certain extent to see the corresponding changes in the computational results of the model. This approach is convenient to be applied but extremely time-consuming. Therefore, in the present study, we adopted a more systematic and economical approach, concentration sensitivity analysis, in a box model to reveal the dependence of ozone and bromine species on the initial mixing ratio of each species in the troposphere. In the concentration sensitivity analysis, the percentage change of the mixing ratio of specified species such as ozone caused by 1% change in the initial species concentration is computed, which identifies the importance of each chemical species in the initial composition of the atmosphere for the depletion of ozone in the Arctic spring.

The structure of the manuscript is organized as follows. In Sect. 2, the mathematical equations used in the present study are given. The configuration of the model is also presented in this section. Later, most of the computational results are shown in Sect. 3. The importance of each initial species concentration for the mixing ratios of ozone and bromine species during ODEs is indicated by the values of the sensitivity coefficients. At the end of this section, we modify the initial mixing ratios of the most influential species which are discovered by the concentration sensitivity analysis to make a comparison between the simulation results before and after the modification. At last, in Sect. 4, major conclusions obtained in the present study are given. Future improvements of the present model are also discussed.

2. Mathematical Models and Methods

The chemical reaction system used in the present study can be expressed as

$$\frac{\mathrm{d}\vec{c}}{\mathrm{d}t} = \vec{f}(\vec{c}, \vec{k}) + \vec{E}, \tag{1}$$

with the initial condition $\vec{c}|_{t=0} = \vec{c^0}$. In Eq. (1), $\vec{c}$ is a column vector consisting of species concentrations, and its i-th element, c_i, denotes the concentration of the i-th species. $\vec{k}$ in Eq. (1) represents a vector of reaction rate constants, and its j-th element, k_j, corresponds to the rate coefficient of the j-th reaction. t in Eq. (1) denotes time, and $\vec{E}$ is the source term for the local emissions from the underlying surface. After implementing a reaction mechanism of ODEs in a box model KINAL [21] and solving Eq. (1), we are able to capture the temporal evolutions of ozone and principal bromine species in the ODE event. The adopted reaction mechanism in the present study is taken from previous studies [13,17,22] which consists of 92 reactions among 39 chemical species. The full reaction mechanism is listed in Tab. A1 of the Appendix, and this mechanism includes both the gaseous reactions and the heterogeneous reactions occuring on the surfaces of polar substrates. The rate coefficients of the gas-phase reactions are estimated by using the Arrhenius equation [23] based on the latest kinetic data for atmospheric chemistry [24]. A constant temperature 258 K is also assumed for the calculation of the gas-phase reaction rates in the mechanism [13]. In contrast to that, the estimation of the rates of the heterogeneous reactions depends on the meteorological parameters such as the wind speed and the stability of the boundary layer. Parameterizations from previous model studies [13,17,22] for these heterogeneous reactions are adopted in the present study. In these parameterizations, heights of the boundary layer and the surface layer need to be prescribed. In the present box model study, a typical polar boundary layer height, 200 m, is used for defining the top of the computational domain, and the height of the surface layer is assumed as 10% of the boundary layer height, i.e. 20 m [25].

The initial composition of the atmosphere used in the model is listed in Tab. 1, which represents a typical Arctic condition. A small amount of bromine (0.3 ppt Br_2 and 0.01 ppt HBr) is prescribed in the model which plays the role of triggering the bromine explosion mechanism. Nitrogen oxides (NO_x), HONO, H_2O_2 and HCHO were found to be emitted from the underlying surfaces of polar regions [26–29]. Thus, fluxes of these species emitted from the ice/snow-covered surfaces of Arctic are also included in the model (see Tab. 2). The emission rates of these species are estimated according to previous measurements [26–29], and the emission of HONO is assumed to be equal to that of NO_2 [28].

After the initialization of the model, Eq. (1) is solved in the subroutine DIFF of the box model KINAL with the implementation of a fourth-order semi-implicit Runge-Kutta scheme [30]. Then

Table 1. Initial atmospheric composition in the boundary layer (ppm = parts per million, ppb = parts per billion, ppt = parts per trillion) [17].

Species	Mixing ratio	Species	Mixing ratio
O_3	40 ppb	C_2H_6	2.5 ppb
Br_2	0.3 ppt	C_2H_4	100 ppt
HBr	0.01 ppt	C_2H_2	600 ppt
CH_4	1.9 ppm	C_3H_8	1.2 ppb
CO_2	371 ppm	NO	5 ppt
CO	132 ppb	NO_2	10 ppt
HCHO	100 ppt	H_2O	800 ppm
CH_3CHO	100 ppt		

Table 2. Emission fluxes from the ice/snow-covered ground surface [17].

Species	Emission rates [molec. cm^{-2} s^{-1}]	Reference
NO	1.6×10^7	Jones *et al.* [26,27]
NO_2	1.6×10^7	Jones *et al.* [26,27]
HONO	1.6×10^7	Grannas *et al.* [28]
H_2O_2	1.0×10^8	Jacobi *et al.* [29]
HCHO	6.0×10^7	Jacobi *et al.* [29]

the temporal behavior of ozone and bromine containing compounds are obtained. Afterward, we performed a concentration sensitivity analysis on the present reaction mechanism to identify the most influential atmospheric components in the initial atmosphere for ozone and bromine species during ODEs. The definition of the concentration sensitivity is as follows,

$$S_{ij}(t) = \frac{\partial c_i(t)}{\partial c_j^0}. \tag{2}$$

In Eq. (2), $c_i(t)$ is the concentration of the i-th chemical species at the time t, and c_j^0 denotes the initial concentration of the j-th species. S_{ij} in Eq. (2) is the absolute concentration sensitivity, which shows the ratio between the change of the mixing ratio of the i-th species and the variation in the initial concentration of the j-th atmospheric component. However, the absolute concentration sensitivity is inapplicable for identifying the most important initial components of the atmosphere as the magnitude of the variations in the initial components differs significantly. Therefore, in order to compare the sensitivity coefficients belonging to different initial chemical species, we normalized the absolute sensitivity by multiplying S_{ij} with c_j^0/c_i, thus obtaining the relative concentration sensitivity $\widetilde{S}_{ij}$, which can be denoted as

$$\widetilde{S}_{ij}(t) = \frac{\partial \ln c_i(t)}{\partial \ln c_j^0} = \frac{c_j^0}{c_i(t)} \frac{\partial c_i(t)}{\partial c_j^0}. \tag{3}$$

In Eq. (3), the relative concentration sensitivity $\widetilde{S}_{ij}$ is a dimensionless parameter which represents the percentage change in i-th species concentration due to 1% change of the initial concentration of the j-th species. Thus, the importance of the initial concentration belonging to each component of the atmosphere for the mixing ratios of ozone and bromine species during ODEs is revealed by the relative concentration sensitivity. In KINAL, the relative concentration sensitivity is computed in the subroutine SENS by using a Decomposed Direct Method [31], which has been proved robust and highly efficient [32].

After obtaining the relative concentration sensitivity on each initial component of the atmosphere, we chose the species with the largest sensitivities to perform a following investigation. The initial mixing ratios of these important species are multiplied by a factor of 1.5 or divided by 2 to observe the corresponding changes of the kinetic system. In the present study, we focus on the deviations in the mixing ratios of ozone and three principal bromine species (BrO, HOBr andBr) during the ODE event.

In the next section, the computational results are shown and discussed.

3. Results and Discussion

In this section, we first show the temporal evolution of the principal chemical species such as ozone in the 200 m boundary layer during the ODE. Then the relative concentration sensitivities of

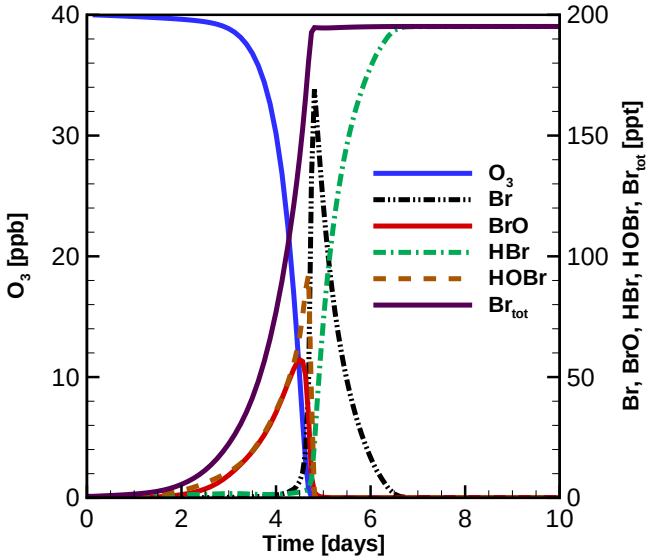

Figure 1. Temporal evolution of ozone and principal bromine species in a 200 m boundary layer with the original initial atmospheric composition [17,22].

ozone, BrO and HOBr on the initial mixing ratios of the atmospheric components are displayed. At last, the initial concentrations of the most influential species are varied so that the response of the system is captured and discussed.

3.1. Temporal Evolution of Ozone and Principal Bromine Species

Figure 1 shows the development of the mixing ratios of ozone and principal bromine species with time. Since this result has been presented and discussed in our previous publications [17,22], in this manuscript, we only give a brief introduction to important features of this simulation. It is seen in Fig. 1 that ozone starts to drop significantly after day 3 before which the ozone depletion rate is less than 0.1 ppb h^{-1}. In the early stage of the simulation (before day 3), as ozone is abundant in the boundary layer, the formation of BrO is able to proceed. Therefore, BrO and HOBr increase steadily, which makes them the major contributions to the total bromine amount in the troposphere. In contrast to that, since Br atoms react with ozone rapidly, in the presence of ozone at this early time stage, Br atoms can be hardly observed. After day 3, HOBr reaches its peak value of 92 ppt. Consequently, the activation of bromide from the ice/snow-covered surface is strongly enhanced. As a result, the total bromine amount in the ambient air increases explosively, thus speeding up the depletion of ozone. The rate of ozone depletion in this time period exceeds 0.1 ppb h^{-1}, and reaches the maximum of 1.9 ppb h^{-1}. On day 4.6, when ozone drops to a level lower than 10% of its background value (4 ppb). The formation of BrO tends to be prohibited. Thus, the mixing ratios of BrO and HOBr decline instantly to a value lower than 1 ppt. Due to the photolysis decomposition of BrO, Br builds up to be the major bromine species and amounts to 170 ppt on approximately day 4.8. Later on, this amount of Br atoms is converted to HBr through the scavenging process by aldehydes in the troposphere. HBr thus becomes the major bromine species remaining in the boundary layer after the ODE, which is in accordance with the previous measurement [33].

In the next section, a concentration sensitivity analysis is applied on the present reaction mechanism for the time period during the depletion of ozone.

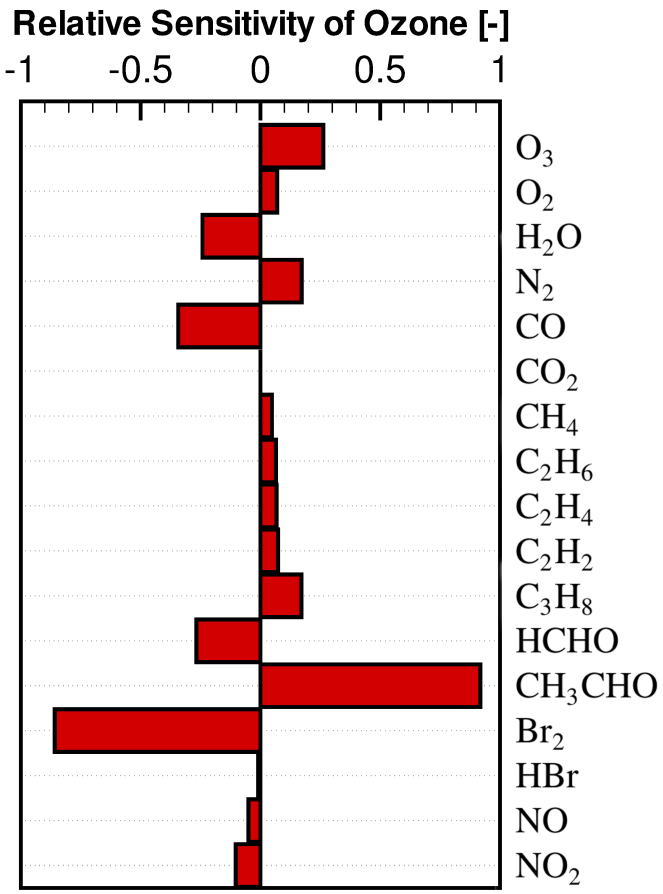

Figure 2. Relative concentration sensitivities of ozone on the initial mixing ratio of each component in the troposphere (on day 4).

3.2. Concentration Sensitivity Analysis of the Mixing Ratios of Ozone and Bromine Containing Compounds during the ODE

Figure 2 displays the relative concentration sensitivities of ozone in the ambient air on day 4 which resides in the depletion period of ozone on each component of the initial atmospheric composition. It is seen that for the ozone mixing ratio during the ODE, the initial concentration of CH_3CHO has the largest absolute value of the relative concentration sensitivity, which means that the ozone during the ODE is mostly influenced by the initial concentration of CH_3CHO. Besides, the sign of the sensitivity coefficient corresponding to CH_3CHO is positive, which denotes that the increase of the initial concentration of CH_3CHO tends to enhance the ozone mixing ratio during ODEs. The reason is attributable to the absorption of Br by CH_3CHO:

$$\mathrm{Br} + \mathrm{CH_3CHO} \xrightarrow{\mathrm{O_2}} \mathrm{HBr} + \mathrm{CH_3CO_3}. \quad \text{(R5)}$$

As Br is a chemical species which directly consumes ozone, when the initial concentration of CH_3CHO increases, the quantity of Br available for the consumption of ozone during ODEs becomes less. As a result, the depletion of ozone is retarded, and the mixing ratio of ozone would increase. In contrast to that, it is interesting to note that the sensitivity coefficient of ozone for HCHO has a negative value on day 4 (see Fig. 2). It denotes that different from CH_3CHO, the increase of the initial concentration of HCHO would decrease the mixing ratio of ozone and thus speed up the ODE.

By comparing the reactions related to CH_3CHO and HCHO in the mechanism used in the present study, we found that for CH_3CHO, reaction (R5) is the major chemical pathway which influences the ozone mixing ratio heavily. As discussed above, through reaction (R5), the active bromine atoms are scavenged by CH_3CHO and converted to HBr, leading to the slow down of the ODE. However, for HCHO, the reaction between HCHO and Br is as follows,

$$Br + HCHO \xrightarrow{O_2} HBr + CO + HO_2. \quad (R6)$$

Although Br is also converted to the inert bromine species HBr through reaction (R6), CO and HO_2 are produced. As CO is able to react with hydroxyl radicals (OH) in the troposphere and then forms HO_2, the total amount of HO_2 in the troposphere is strongly enhanced during ODEs when reaction (R6) proceeds. Since HO_2 is capable of oxidizing BrO to HOBr, the increase of the initial mixing ratio of HCHO would strengthen the formation of HOBr, thus speeding up the bromine explosion mechanism. As a result, the depletion of ozone is accelerated.

The second important initial component of the troposphere for the ozone mixing ratio during ODEs is Br_2 according to the sensitivity values shown in Fig. 2. This is not entirely surprising as the initial Br_2 plays the role of stimulating the bromine explosion mechanism which consequently leads to the consumption of ozone. Thus, the increase of the initial Br_2 in the atmosphere would significantly speed up the occurrence of ODEs. In contrast to Br_2, the sensitivity of the ozone mixing ratio on HBr is negligible. This is because that HBr is inert in the reaction cycle of the ozone depletion and the associated bromine explosion mechanism as it can be hardly reactivated and photolyzed. The chemical species CO also has a relatively large sensitivity among the initial components of the atmosphere, which is attributable to the speedup of the bromine explosion mechanism via the reactions:

$$CO + OH \xrightarrow{O_2} CO_2 + HO_2, \quad (R7)$$

$$HO_2 + BrO \rightarrow HOBr + O_2, \quad (R8)$$

which has been discussed above. Apart from these species, the initial mixing ratio of water vapor (H_2O) has a negative sensitivity as it is the major sink of the O_x family ($O_3 + O(^1D)$) in the troposphere [2]. It is also interesting to note that the mixing ratio of ozone during ODEs depends negatively on the initial concentrations of nitrogen oxides ($NO + NO_2$), which means that the role of the nitrogen oxides during ODEs is to accelerate the ODE and decrease the ozone mixing ratio instead of forming ozone. This ozone-consumption effect brought about by nitrogen oxides during ODEs is caused by the hydrolysis of $BrONO_2$,

$$BrONO_2 + H_2O \xrightarrow{mp} HOBr + HNO_3, \quad (R9)$$

in which HOBr is formed. As a result, the bromine explosion and the following ozone consumption are enhanced in the presence of nitrogen oxides. This finding is also in consistence with our previous box model study [17] in which the addition of the nitrogen chemistry is found to advance the ODE.

The relative concentration sensitivities of BrO on each component of the initial atmospheric composition are displayed in Fig. 3. Compared to the results shown in Fig. 2, all the components except ozone have an opposite sign of the sensitivity coefficients. It represents that the formation of BrO is correlated with the decline of ozone. Besides, it is shown in Fig. 3 that the sensitivity coefficient of BrO on the initial mixing ratio of ozone is relatively large and possesses a positive sign. It is expectable as the major formation pathway of BrO is the reaction $Br + O_3 \rightarrow BrO + O_2$, which requires the presence of ozone. These findings are in agreement with the conclusions obtained by Hausmann and Platt [34], suggesting that BrO is an important indicator of ODEs as the enhancement of BrO requires the presence of ozone and the drop of the ozone mixing ratio.

At the end of this section, attentions are paid to the relative concentration sensitivities of HOBr on the initial atmospheric composition (see Fig. 4). It is found that the results obtained for HOBr are similar to those for BrO shown in Fig. 3. However, the initial concentrations of CH_4, C_2H_4 and

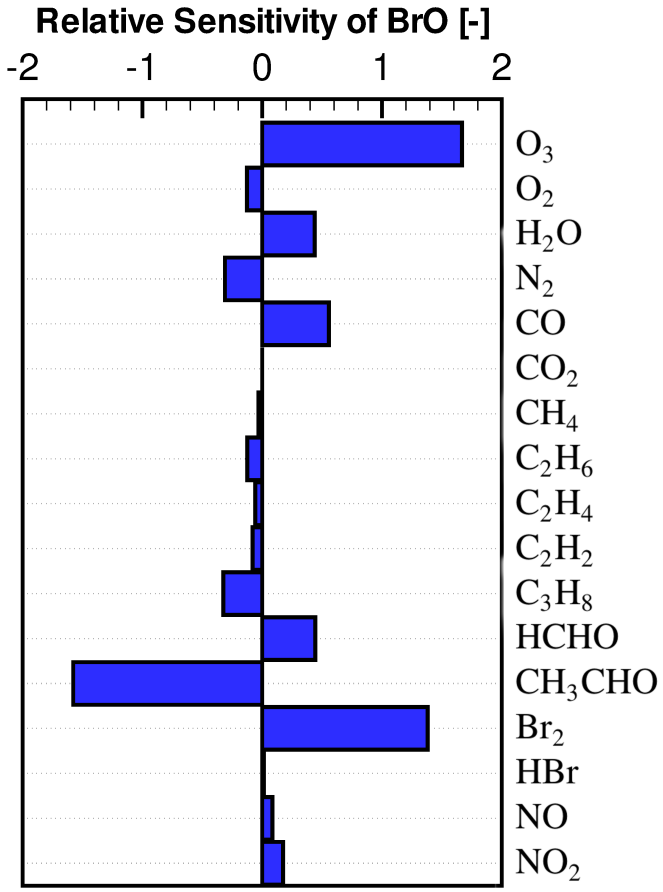

Figure 3. Relative concentration sensitivities of BrO on the initial mixing ratio of each component in the troposphere (on day 4).

C_2H_2 have positive sensitivities for the HOBr mixing ratio while negative values are obtained for the mixing ratio of BrO. By investigating the reaction mechanism used in the present study, we found that for CH_4, it participates in a reaction sequence as follows:

$$CH_4 + OH \xrightarrow{O_2} CH_3O_2 + H_2O, \tag{R10}$$

$$CH_3O_2 + BrO \rightarrow HOBr + HCHO + 0.5O_2. \tag{R11}$$

Therefore, through reactions (R10) and (R11), BrO is converted to HOBr, which explains the different signs of the sensitivity coefficients for the mixing ratios of BrO and HOBr. With respect to C_2H_4 and C_2H_2, these two species are involved in the following reactions:

$$Br + C_2H_4 \xrightarrow{2.5O_2} 2CO + HO_2 + HBr + H_2O, \tag{R12}$$

and

$$Br + C_2H_2 \xrightarrow{2O_2} 2CO + HO_2 + HBr. \tag{R13}$$

In these two reactions, not only the major reactant of BrO, Br atoms, are consumed, but also HO_2 is formed. As HO_2 is able to oxidize BrO to HOBr, these two reactions with the involvement of C_2H_4

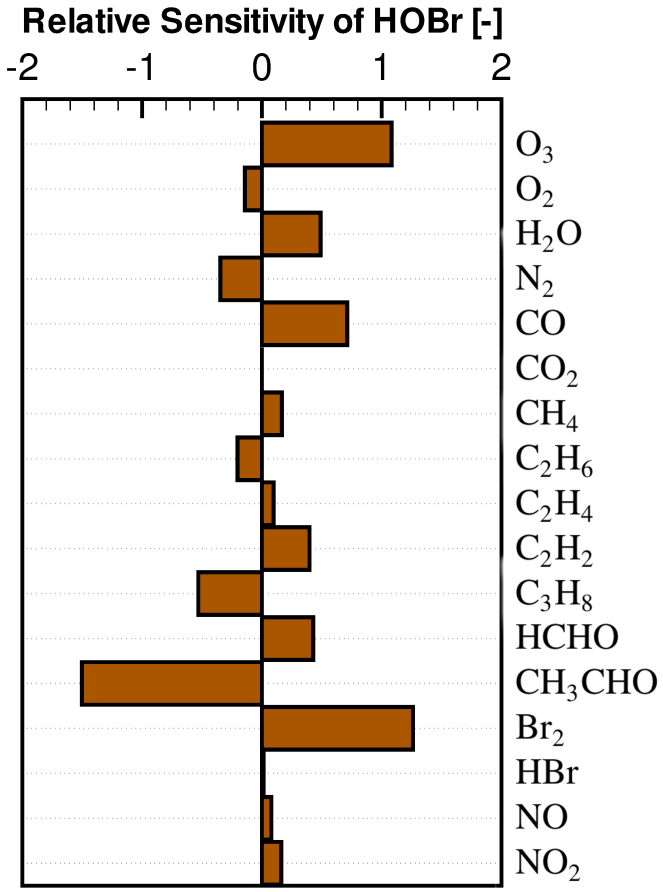

Figure 4. Relative concentration sensitivities of HOBr on the initial mixing ratio of each component in the troposphere (on day 4).

and C_2H_2 cause a speciation shift from BrO to HOBr, leading to negative sensitivities of these two species for BrO and positive sensitivities for HOBr.

Next, we chose the most influential species which are identified in the concentration sensitivity analysis, CH_3CHO, Br_2 and C_2H_2, to perform numerical tests by multiplying their initial mixing ratios by 1.5 and 0.5 to study the corresponding changes in the concentrations of ozone and principal bromine species.

3.3. Evolution of Ozone, BrO, HOBr and Br with Different Initial Atmospheric Composition

Figure 5 shows the temporal behavior of ozone and principal bromine species (BrO, HOBr and Br) before and after the modification of the initial mixing ratio of CH_3CHO. It is clearly seen in Fig. 5(a) that the change in the initial CH_3CHO mixing ratio causes a significant acceleration or retardation of the ODE. The ozone in the 200 m boundary layer declines to a level lower than 4 ppb on day 4 and day 5.5 when the initial mixing ratio of CH_3CHO is changed to 50 ppt and 150 ppt, respectively. However, from Fig. 5(a), it is also found that the acceleration or deceleration of the ODE is mostly attributable to the shortening of the induction stage which resides before the significant decline of ozone. The simulated ozone depletion rates under different initial conditions are similar. Meanwhile, in Figs. 5(b), (c) and (d), we found that although the increase of the bromine species such as BrO and HOBr are advanced or delayed after the modification of the initial CH_3CHO, the peak values of the principal bromine species during ODEs are approximately equal to that before the

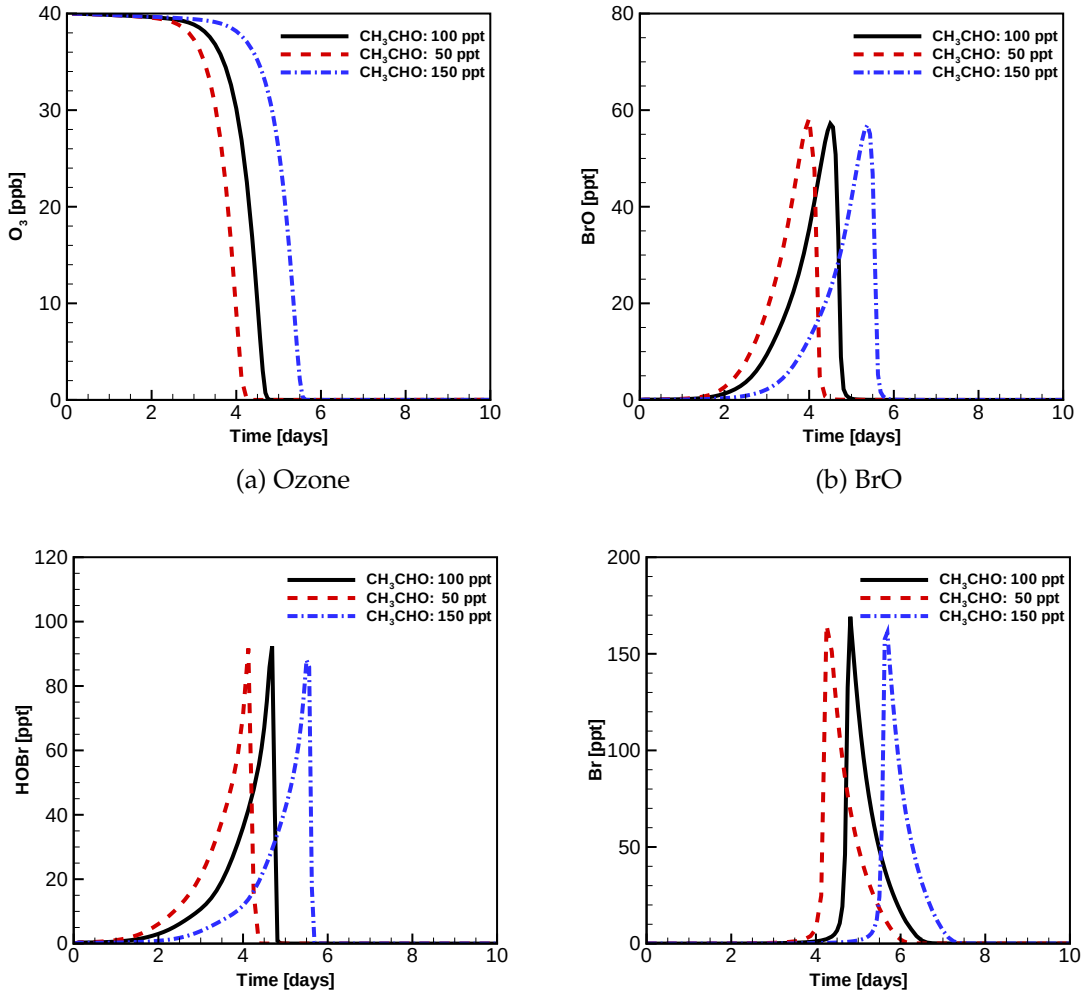

(a) Ozone (b) BrO

(c) HOBr (d) Br

Figure 5. Simulated Evolution of ozone, BrO, HOBr and Br over 10 days with 3 different initial CH_3CHO mixing ratios (100 ppt (solid line), 150 ppt (dash line) and 50 ppt (dash dot line)).

modification. Therefore, we conclude that the change in the initial mixing ratio of CH_3CHO leads to a variation in the onset of the ODE while the depletion rate of ozone and the peak values of the principal bromine species during ODEs are only slightly influenced.

Simulation results after changing the initial mixing ratio of Br_2 from 0.3 ppt to 0.15 ppt and 0.45 ppt are also obtained (not shown here). We found that the effects on the mixing ratios of ozone and bromine species caused by the modification of the initial Br_2 are similar to those with the modification of the initial CH_3CHO shown in Fig. 5. It is observed that when the initial Br_2 is reduced from the original value 0.3 ppt to 0.15 ppt, the depletion of ozone occurs one day later than that with the original Br_2 value, starting on approximately day 4. In contrast to that, a prescribed 0.45 ppt Br_2 in the initial composition of the troposphere leads to an advancement of the ODE, which occurs on approximately day 2.6. However, similar to the simulation scenario for the investigation of CH_3CHO, little has changed about the peak values of principal bromine species and the depletion rate of ozone after the variation in the initial mixing ratio of Br_2.

At last, we chose a special chemical species indicated in the concentration sensitivity analysis, C_2H_2, to perform the numerical tests. It is seen in Fig. 2 and Fig. 3 that the relative concentration sensitivities of ozone and BrO on the initial mixing ratio of C_2H_2 are lower than 0.1, which represents

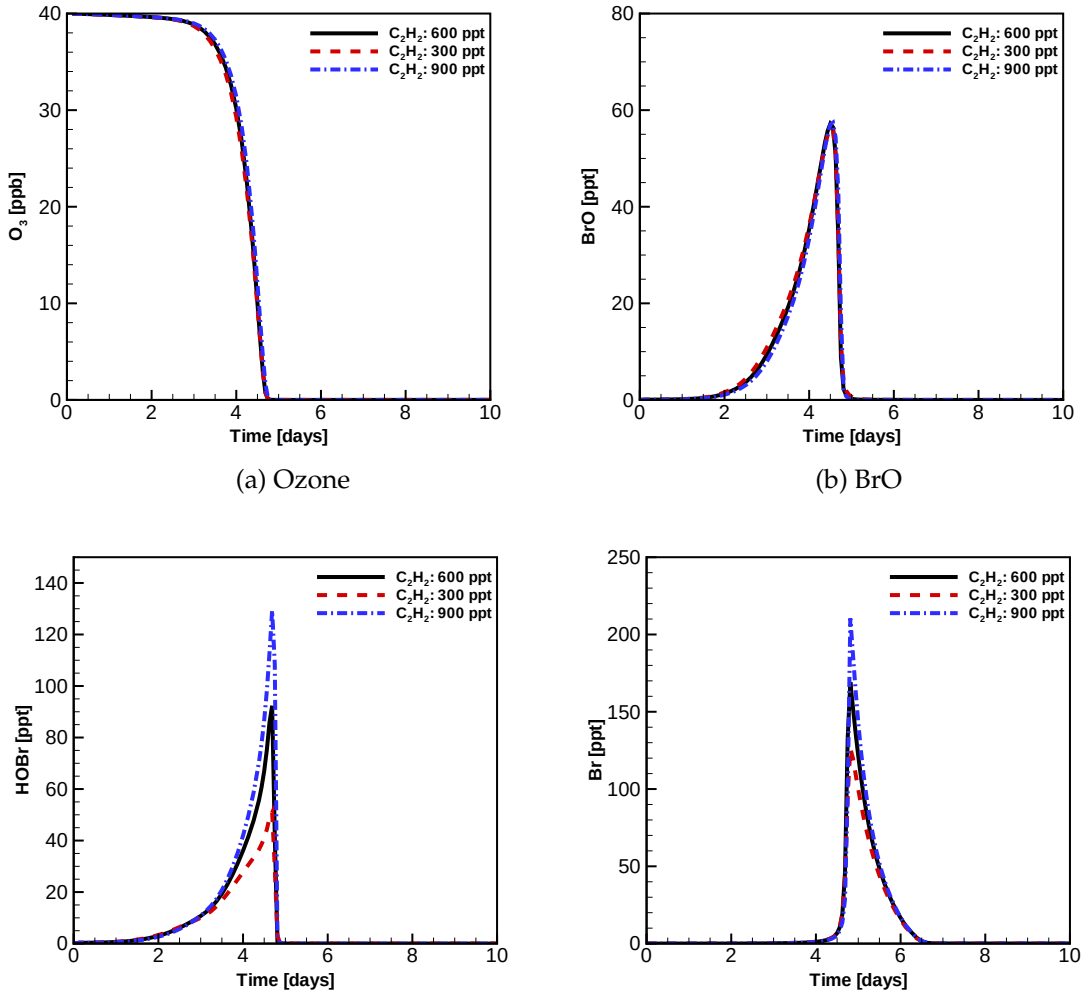

(a) Ozone (b) BrO

(c) HOBr (d) Br

Figure 6. Simulated Evolution of ozone, BrO, HOBr and Br over 10 days with 3 different initial C_2H_2 mixing ratios (600 ppt (solid line), 300 ppt (dash line) and 450 ppt (dash dot line)).

that the mixing ratios of ozone and BrO during ODEs are slightly influenced by the initial C_2H_2. However, in Fig. 4, C_2H_2 possesses a sensitivity coefficient of approximately 0.4. It indicates that the HOBr mixing ratio during ODEs depends heavily on the initial C_2H_2. Thus, we modified the initial mixing ratio of C_2H_2 from the original value 600 ppt to 300 ppt and 900 ppt and observed the outcome of the simulation (see Fig. 6). It is seen in Figs. 6(a) and (b) that the depletion of ozone and the temporal behavior of BrO after the modifications are almost identical to those with the original value of the initial C_2H_2, which is also in agreement with the results obtained in the sensitivity analysis. In contrast to that, the increase of the initial mixing ratio of C_2H_2 leads to a significant rise up of HOBr and Br levels (see Figs. 6(c) and (d)). Under the condition of 600 ppt initial C_2H_2, HOBr and Br amount to maximum of 129 ppt and 210 ppt, respectively. Besides, when the initial C_2H_2 is reduced to 300 ppt, the peak values of HOBr and Br drop to 51 ppt and 126 ppt, which are only 40% and 60% of the values in the simulation with 600 ppt initial C_2H_2. To summary, according to the present simulation results, we can say that the mixing ratio of C_2H_2 in the troposphere would not affect the depletion of ozone and the temporal change of BrO significantly, but the amount of HOBr and Br atoms in the troposphere during ODEs are critically determined by the C_2H_2 concentration.

4. Conclusions and Future Developments

In the present study, a sensitivity analysis is applied on a reaction mechanism representing the ozone depletion and the associated bromine explosion in the Arctic spring. The dependence of the mixing ratios of ozone and principal bromine species on the initial composition of the atmosphere in the polar boundary layer is revealed. It is found that for the ozone mixing ratio during the ODE, the initial concentration of CH_3CHO is the most deterministic factor which critically controls the depletion rate of ozone. The reason for the relative importance of CH_3CHO is attributable to the absorption of Br atoms by the initial CH_3CHO, which reduces the reactive bromine in the troposphere and slows down the ozone depletion. In contrast to that, although Br is also scavenged by HCHO, the formation of HO_2 is enhanced in the presence of HCHO. As a result, the oxidation of BrO and the associated bromine explosion mechanism with the involvement of HOBr are strengthened by the increase of the initial concentration of HCHO, leading to a speedup of the ODE, which is also indicated by the negative ozone sensitivity coefficient on HCHO. Besides, CH_4, C_2H_4 and C_2H_2 are shown to cause a speciation shift from BrO to HOBr, which causes an opposite sign of the sensitivity coefficients of these species for BrO and HOBr.

After changing the initial concentrations of CH_3CHO and Br_2 in simulations, we found that the onset of the ODE is strongly influenced by the modification of the initial mixing ratios of these two species. However, the rate of ozone depletion and the peak values of principal bromine species such as BrO and HOBr are as similar as those before the modification. In contrast, the increase of the initial concentration of C_2H_2 exerts negligible influence on shortening the induction time of the ODE. Besides, the development of BrO with time is found less dependent on the C_2H_2 concentration. However, the peak values of HOBr and Br during ODEs are found to be critically controlled by the initial mixing ratio of C_2H_2.

The present study has its limitations. For instance, the present sensitivity analysis can be only performed on the species with a non-zero value of the initial mixing ratio due to the definition of the relative concentration sensitivity in the form of Eq. (3). However, it would be helpful that the dependence of the ODE and the bromine explosion mechanism on the initial mixing ratios of all the chemical species included in the model can be estimated. Currently, the authors are developing a modified relative concentration sensitivity analysis so that the relative importance of each component in the troposphere on the ODE can be revealed, which is attributed to a future work.

Acknowledgments: This work was financially supported by the National Natural Science Foundation of China (No. 41375044), the Natural Science Foundation of Jiangsu Province (No. 2015s042), the Double Innovation Talent Program (No. R2015SCB02), the Polar Strategic Foundation (No. 20150308) and the Startup Foundation for Introducing Talent of NUIST (No. 2014r066).

Author Contributions: L. Cao conceived and designed the simulation scenarios, and also performed the computations. N. W. Cao analyzed the concentration sensitivity data and gave valuable suggestions. L. Cao and M. He wrote the paper.

Conflicts of Interest: The authors declare no conflict of interest.

Appendix

Table A1. The complete chemical reaction mechanism with an assumption of a 200 m boundary layer. A constant temperature $T = 258\,K$ is assumed in the model, and the rate of third-body reactions is estimated as $k = k_\infty \times \frac{k_0/k_\infty}{(1+k_0/k_\infty)} \times F_c^{\frac{1}{1+(\log_{10}(k_0/k_\infty))^2}}$ [24].

Reaction Number	Reaction	k $[(\text{molec. cm}^{-3})^{1-n}\text{s}^{-1}]$	Order n	Reference
(R1)	$O_3 + h\nu \rightarrow O(^1D) + O_2$	4.70×10^{-7}	1	Lehrer *et al.* [13]
(R2)	$O(^1D) + O_2 \rightarrow O_3$	$3.20 \times 10^{-11}\exp(67/T)$	2	Atkinson *et al.* [24]
(R3)	$O(^1D) + N_2 \rightarrow O_3 + N_2$	$1.80 \times 10^{-11}\exp(107/T)$	2	Atkinson *et al.* [24]
(R4)	$O(^1D) + H_2O \rightarrow 2OH$	2.20×10^{-10}	2	Atkinson *et al.* [24]
(R5)	$Br + O_3 \rightarrow BrO + O_2$	$1.70 \times 10^{-11}\exp(-800/T)$	2	Atkinson *et al.* [24]
(R6)	$Br_2 + h\nu \rightarrow 2Br$	0.021	1	Lehrer *et al.* [13]
(R7)	$BrO + h\nu \xrightarrow{O_2} Br + O_3$	0.014	1	Lehrer *et al.* [13]
(R8)	$BrO + BrO \rightarrow 2Br + O_2$	2.70×10^{-12}	2	Atkinson *et al.* [24]
(R9)	$BrO + BrO \rightarrow Br_2 + O_2$	$2.90 \times 10^{-14}\exp(840/T)$	2	Atkinson *et al.* [24]
(R10)	$BrO + HO_2 \rightarrow HOBr + O_2$	$4.5 \times 10^{-12}\exp(500/T)$	2	Atkinson *et al.* [24]
(R11)	$HOBr + h\nu \rightarrow Br + OH$	3.00×10^{-4}	1	Lehrer *et al.* [13]
(R12)	$CO + OH(+M) \xrightarrow{O_2} HO_2 + CO_2(+M)$	$1.44 \times 10^{-13}(1 + \frac{[N_2]}{4\times10^{19}})$	2	Atkinson *et al.* [24]
(R13)	$Br + HO_2 \rightarrow HBr + O_2$	$7.70 \times 10^{-12}\exp(-450/T)$	2	Atkinson *et al.* [24]
(R14)	$HOBr + HBr \xrightarrow{aerosol} Br_2 + H_2O$	$(\frac{r}{D_g} + \frac{4}{v_{therm}\gamma})^{-1}\alpha_{eff,aerosol}$		Cao *et al.* [17]
(R15)	$HOBr + H^+ + Br^- \xrightarrow{ice} Br_2 + H_2O$	$(r_a + r_b + r_c)^{-1}\alpha_{eff,ice}$		Cao *et al.* [17]
(R16)	$Br + HCHO \xrightarrow{O_2} HBr + CO + HO_2$	$7.70 \times 10^{-12}\exp(-580/T)$	2	Atkinson *et al.* [24]
(R17)	$Br + CH_3CHO \xrightarrow{O_2} HBr + CH_3CO_3$	$1.80 \times 10^{-11}\exp(-460/T)$	2	Atkinson *et al.* [24]
(R18)	$Br_2 + OH \rightarrow HOBr + Br$	$2.0 \times 10^{-11}\exp(240/T)$	2	Atkinson *et al.* [24]
(R19)	$HBr + OH \rightarrow H_2O + Br$	$5.50 \times 10^{-12}\exp(205/T)$	2	Atkinson *et al.* [24]
(R20)	$Br + C_2H_2 \xrightarrow{3O_2} 2CO + 2HO_2 + Br$	4.20×10^{-14}	2	Borken [35]
(R21)	$Br + C_2H_2 \xrightarrow{2O_2} 2CO + HO_2 + HBr$	8.92×10^{-14}	2	Borken [35]
(R22)	$Br + C_2H_4 \xrightarrow{3.5O_2} 2CO + 2HO_2 + Br + H_2O$	2.52×10^{-13}	2	Barnes *et al.* [36]
(R23)	$Br + C_2H_4 \xrightarrow{2.5O_2} 2CO + HO_2 + HBr + H_2O$	5.34×10^{-13}	2	Barnes *et al.* [36]
(R24)	$CH_4 + OH \xrightarrow{O_2} CH_3O_2 + H_2O$	$1.85 \times 10^{-12}\exp(-1690/T)$	2	Atkinson *et al.* [24]
(R25)	$BrO + CH_3O_2 \rightarrow Br + HCHO + HO_2$	1.60×10^{-12}	2	Aranda *et al.* [37]
(R26)	$BrO + CH_3O_2 \rightarrow HOBr + HCHO + 0.5O_2$	4.10×10^{-12}	2	Aranda *et al.* [37]
(R27)	$OH + O_3 \rightarrow HO_2 + O_2$	$1.70 \times 10^{-12}\exp(-940/T)$	2	Atkinson *et al.* [24]
(R28)	$OH + HO_2 \rightarrow H_2O + O_2$	$4.80 \times 10^{-11}\exp(250/T)$	2	Atkinson *et al.* [24]
(R29)	$OH + H_2O_2 \rightarrow HO_2 + H_2O$	$2.90 \times 10^{-12}\exp(-160/T)$	2	Atkinson *et al.* [24]
(R30)	$OH + OH \xrightarrow{O_2} H_2O + O_3$	$6.20 \times 10^{-14}(T/298)^{2.6}\exp(945/T)$	2	Atkinson *et al.* [24]
(R31)	$HO_2 + O_3 \rightarrow OH + 2O_2$	$2.03 \times 10^{-16}(T/300)^{4.57}\exp(693/T)$	2	Atkinson *et al.* [24]
(R32)	$HO_2 + HO_2 \rightarrow O_2 + H_2O_2$	$2.20 \times 10^{-13}\exp(600/T)$	2	Atkinson *et al.* [24]
(R33)	$C_2H_6 + OH \rightarrow C_2H_5 + H_2O$	$6.90 \times 10^{-12}\exp(-1000/T)$	2	Atkinson *et al.* [24]
(R34)	$C_2H_5 + O_2 \rightarrow C_2H_4 + HO_2$	3.80×10^{-15}	2	Atkinson *et al.* [24]

Reaction Number	Reaction	k $[(\text{molec. cm}^{-3})^{1-n}\text{s}^{-1}]$	Order n	Reference
(R35)	$C_2H_5 + O_2(+M) \rightarrow C_2H_5O_2(+M)$	$k_0 = 5.90 \times 10^{-29}(T/300)^{-3.8}[N_2]$ $k_\infty = 7.80 \times 10^{-12}$ $F_c = 0.58\exp(-T/1250)$ $+0.42\exp(-T/183)$	2	Atkinson *et al.* [24]
(R36)	$C_2H_4 + OH(+M) \xrightarrow{1.5O_2} CH_3O_2 + CO + H_2O(+M)$	$k_0 = 8.60 \times 10^{-29}(T/300)^{-3.1}[N_2]$ $k_\infty = 9.00 \times 10^{-12}(T/300)^{-0.85}$ $F_c = 0.48$	2	Atkinson *et al.* [24]
(R37)	$C_2H_4 + O_3 \rightarrow HCHO + CO + H_2O$	4.33×10^{-19}	2	Sander *et al.* [38]
(R38)	$C_2H_2 + OH(+M) \xrightarrow{1.5O_2} HCHO + CO + HO_2(+M)$	$k_0 = 5.00 \times 10^{-30}(T/300)^{-1.5}[N_2]$ $k_\infty = 1.00 \times 10^{-12}$ $F_c = 0.37$	2	Atkinson *et al.* [24]
(R39)	$C_3H_8 + OH \xrightarrow{2O_2} C_2H_5O_2 + CO + 2H_2O$	$7.60 \times 10^{-12}\exp(-585/T)$	2	Atkinson *et al.* [24]
(R40)	$HCHO + OH \xrightarrow{O_2} CO + H_2O + HO_2$	$5.40 \times 10^{-12}\exp(135/T)$	2	Atkinson *et al.* [24]
(R41)	$CH_3CHO + OH \xrightarrow{O_2} CH_3CO_3 + H_2O$	$4.40 \times 10^{-12}\exp(365/T)$	2	Atkinson *et al.* [24]
(R42)	$CH_3O_2 + HO_2 \rightarrow CH_3O_2H + O_2$	$3.42 \times 10^{-13}\exp(780/T)$	2	Atkinson *et al.* [24]
(R43)	$CH_3O_2 + HO_2 \rightarrow HCHO + H_2O + O_2$	$3.79 \times 10^{-14}\exp(780/T)$	2	Atkinson *et al.* [24]
(R44)	$CH_3OOH + OH \rightarrow CH_3O_2 + H_2O$	$1.00 \times 10^{-12}\exp(190/T)$	2	Atkinson *et al.* [24]
(R45)	$CH_3OOH + OH \rightarrow HCHO + OH + H_2O$	$1.90 \times 10^{-12}\exp(190/T)$	2	Atkinson *et al.* [24]
(R46)	$CH_3OOH + Br \rightarrow CH_3O_2 + HBr$	$2.66 \times 10^{-12}\exp(-1610/T)$	2	Mallard *et al.* [39]
(R47)	$CH_3O_2 + CH_3O_2 \rightarrow CH_3OH + HCHO + O_2$	$6.29 \times 10^{-14}\exp(365/T)$	2	Atkinson *et al.* [24]
(R48)	$CH_3O_2 + CH_3O_2 \xrightarrow{O_2} 2HCHO + 2HO_2$	$3.71 \times 10^{-14}\exp(365/T)$	2	Atkinson *et al.* [24]
(R49)	$CH_3OH + OH \xrightarrow{O_2} HCHO + HO_2 + H_2O$	$2.42 \times 10^{-12}\exp(-345/T)$	2	Atkinson *et al.* [24]
(R50)	$C_2H_5O_2 + C_2H_5O_2 \rightarrow C_2H_5O + C_2H_5O + O_2$	6.40×10^{-14}	2	Atkinson *et al.* [24]
(R51)	$C_2H_5O + O_2 \rightarrow CH_3CHO + HO_2$	7.44×10^{-15}	2	Sander *et al.* [38]
(R52)	$C_2H_5O + O_2 \rightarrow CH_3O_2 + HCHO$	7.51×10^{-17}	2	Sander *et al.* [38]
(R53)	$C_2H_5O_2 + HO_2 \rightarrow C_2H_5OOH + O_2$	$3.80 \times 10^{-13}\exp(900/T)$	2	Atkinson *et al.* [24]
(R54)	$C_2H_5OOH + OH \rightarrow C_2H_5O_2 + H_2O$	8.21×10^{-12}	2	Sander *et al.* [38]
(R55)	$C_2H_5OOH + Br \rightarrow C_2H_5O_2 + HBr$	5.19×10^{-15}	2	Sander *et al.* [38]
(R56)	$OH + OH(+M) \longrightarrow H_2O_2(+M)$	$k_0 = 6.90 \times 10^{-31}(T/300)^{-0.8}[N_2]$ $k_\infty = 2.60 \times 10^{-11}$ $F_c = 0.50$	2	Atkinson *et al.* [24]
(R57)	$H_2O_2 + h\nu \rightarrow 2OH$	2.00×10^{-6}	1	Lehrer *et al.* [13]
(R58)	$HCHO + h\nu \xrightarrow{2O_2} 2HO_2 + CO$	5.50×10^{-6}	1	Lehrer *et al.* [13]
(R59)	$HCHO + h\nu \rightarrow H_2 + CO$	9.60×10^{-6}	1	Lehrer *et al.* [13]
(R60)	$C_2H_4O + h\nu \rightarrow CH_3O_2 + CO + +HO_2$	6.90×10^{-7}	1	Lehrer *et al.* [13]
(R61)	$CH_3O_2H + h\nu \rightarrow OH + HCHO + HO_2$	1.20×10^{-6}	1	Lehrer *et al.* [13]
(R62)	$C_2H_5O_2H + h\nu \rightarrow C_2H_5O + OH$	1.20×10^{-6}	1	Lehrer *et al.* [13]
(R63)	$NO + O_3 \rightarrow NO_2 + O_2$	$1.40 \times 10^{-12}\exp(-1310/T)$	2	Atkinson *et al.* [24]
(R64)	$NO + HO_2 \rightarrow NO_2 + OH$	$3.60 \times 10^{-12}\exp(270/T)$	2	Atkinson *et al.* [24]
(R65)	$NO_2 + O_3 \rightarrow NO_3 + O_2$	$1.40 \times 10^{-13}\exp(-2470/T)$	2	Atkinson *et al.* [24]
(R66)	$NO_2 + OH(+M) \rightarrow HNO_3(+M)$	$k_0 = 3.30 \times 10^{-30}(T/300)^{-3.0}[N_2]$ $k_\infty = 4.10 \times 10^{-11}$ $F_c = 0.40$	2	Atkinson *et al.* [24]
(R67)	$NO + NO_3 \rightarrow 2NO_2$	$1.80 \times 10^{-11}\exp(110/T)$	2	Atkinson *et al.* [24]
(R68)	$HONO + OH \rightarrow NO_2 + H_2O$	$2.50 \times 10^{-12}\exp(260/T)$	2	Atkinson *et al.* [24]
(R69)	$HO_2 + NO_2(+M) \rightarrow HNO_4(+M)$	$k_0 = 1.80 \times 10^{-31}(T/300)^{-3.2}[N_2]$ $k_\infty = 4.70 \times 10^{-12}$ $F_c = 0.60$	2	Atkinson *et al.* [24]
(R70)	$HNO_4(+M) \rightarrow NO_2 + HO_2(+M)$	$k_0 = 4.10 \times 10^{-5}\exp(-10650/T)[N_2]$ $k_\infty = 4.80 \times 10^{15}\exp(-11170/T)$ $F_c = 0.60$	1	Atkinson *et al.* [24]

Reaction Number	Reaction	k $[(\text{molec. cm}^{-3})^{1-n}\text{s}^{-1}]$	Order n	Reference
(R71)	$HNO_4 + OH \rightarrow NO_2 + H_2O + O_2$	$3.20 \times 10^{-13} \exp(690/T)$	2	Atkinson *et al.* [24]
(R72)	$NO + OH(+M) \rightarrow HONO(+M)$	$k_0 = 7.40 \times 10^{-31}(T/300)^{-2.4}[N_2]$ $k_\infty = 3.30 \times 10^{-11}(T/300)^{-0.3}$ $F_c = 0.81$	2	Atkinson *et al.* [24]
(R73)	$OH + NO_3 \rightarrow NO_2 + HO_2$	2.00×10^{-11}	2	Atkinson *et al.* [24]
(R74)	$HNO_3 + h\nu \rightarrow NO_2 + OH$	4.40×10^{-8}	1	Lehrer *et al.* [13]
(R75)	$NO_2 + h\nu \xrightarrow{O_2} NO + O_3$	3.50×10^{-3}	1	Lehrer *et al.* [13]
(R76)	$NO_3 + h\nu \xrightarrow{O_2} NO_2 + O_3$	1.40×10^{-1}	1	Lehrer *et al.* [13]
(R77)	$NO_3 + h\nu \rightarrow NO + O_2$	1.70×10^{-2}	1	Lehrer *et al.* [13]
(R78)	$NO + CH_3O_2 \xrightarrow{O_2} HCHO + HO_2 + NO_2$	$2.30 \times 10^{-12} \exp(360/T)$	2	Atkinson *et al.* [24]
(R79)	$NO_3 + CH_3OH \xrightarrow{O_2} HCHO + HO_2 + HNO_3$	$9.40 \times 10^{-13} \exp(-2650/T)$	2	Atkinson *et al.* [24]
(R80)	$NO_3 + HCHO \xrightarrow{O_2} CO + HO_2 + HNO_3$	5.60×10^{-16}	2	Atkinson *et al.* [24]
(R81)	$NO + C_2H_5O_2 \xrightarrow{O_2} CH_3CHO + NO_2 + HO_2$	$2.60 \times 10^{-12} \exp(380/T)$	2	Atkinson *et al.* [24]
(R82)	$NO + CH_3CO_3 \xrightarrow{O_2} CH_3O_2 + NO_2 + CO_2$	$7.50 \times 10^{-12} \exp(290/T)$	2	Atkinson *et al.* [24]
(R83)	$NO_2 + CH_3CO_3(+M) \rightarrow PAN(+M)$	$k_0 = 2.70 \times 10^{-28}(T/300)^{-7.1}[N_2]$ $k_\infty = 1.20 \times 10^{-11}(T/300)^{-0.9}$ $F_c = 0.30$	2	Atkinson *et al.* [24]
(R84)	$Br + NO_2(+M) \rightarrow BrNO_2(+M)$	$k_0 = 4.20 \times 10^{-31}(T/300)^{-2.4}[N_2]$ $k_\infty = 2.70 \times 10^{-11}$ $F_c = 0.55$	2	Atkinson *et al.* [24]
(R85)	$Br + NO_3 \rightarrow BrO + NO_2$	1.60×10^{-11}	2	Atkinson *et al.* [24]
(R86)	$BrO + NO_2(+M) \rightarrow BrONO_2(+M)$	$k_0 = 4.70 \times 10^{-31}(T/300)^{-3.1}[N_2]$ $k_\infty = 1.80 \times 10^{-11}$ $F_c = 0.40$	2	Atkinson *et al.* [24]
(R87)	$BrO + NO \rightarrow Br + NO_2$	$8.70 \times 10^{-12} \exp(260/T)$	2	Atkinson *et al.* [24]
(R88)	$BrONO_2 + h\nu \rightarrow NO_2 + BrO$	3.40×10^{-4}	1	Lehrer *et al.* [13]
(R89)	$BrNO_2 + h\nu \rightarrow NO_2 + Br$	9.30×10^{-5}	1	Lehrer *et al.* [13]
(R90)	$BrONO_2 + H_2O \xrightarrow{aerosol} HOBr + HNO_3$	$(\frac{r}{D_g} + \frac{4}{v_{therm}\gamma})^{-1}\alpha_{eff,aerosol}$		Cao *et al.* [17]
(R91)	$PAN + h\nu \rightarrow NO_2 + CH_3CO_3$	6.79×10^{-7}	1	Fishman and Carney [40]
(R92)	$BrONO_2 + H_2O \xrightarrow{ice} HOBr + HNO_3$	$(r_a + r_b + r_c)^{-1}\alpha_{eff,ice}$		Cao *et al.* [17]

References

1. Schoenbein, C. *Recherches sur la nature de l'odeur qui se manifeste dans certaines actions chimiques*; 1840.
2. Seinfeld, J.H.; Pandis, S.N. *Atmospheric Chemistry and Physics: From Air Pollution to Climate Change*; Wiley-Interscience, 2006.
3. Lippmann, M. Health effects of tropospheric ozone. *Environ. Sci. Technol.* **1991**, *25*, 1954–1962.
4. Tropospheric Ozone, the Polluter. http://www.ucar.edu/learn/1_7_1.htm/.
5. Vingarzan, R. A review of surface ozone background levels and trends. *Atmos. Environ.* **2004**, *38*, 3431 – 3442.
6. Oltmans, S.J. Surface ozone measurements in clean air. *Journal of Geophysical Research: Oceans* **1981**, *86*, 1174–1180.
7. Bottenheim, J.; Gallant, A.; Brice, K. Measurements of NO_Y species and O_3 at 82° N latitude. *Geophys. Res. Lett.* **1986**, *13*, 113–116.
8. Barrie, L.A.; Bottenheim, J.W.; Schnell, R.C.; Crutzen, P.J.; Rasmussen, R.A. Ozone destruction and photochemical reactions at polar sunrise in the lower Arctic atmosphere. *Nature* **1988**, *334*, 138–141.
9. Hönninger, G.; Platt, U. Observations of BrO and its vertical distribution during surface ozone depletion at Alert. *Atmos. Environ.* **2002**, *36*, 2481 – 2489.
10. Platt, U.; Hönninger, G. The role of halogen species in the troposphere. *Chemosphere* **2003**, *52*, 325 – 338.
11. Simpson, W.R.; von Glasow, R.; Riedel, K.; Anderson, P.; Ariya, P.; Bottenheim, J.; Burrows, J.; Carpenter, L.J.; Frieß, U.; Goodsite, M.E.; Heard, D.; Hutterli, M.; Jacobi, H.W.; Kaleschke, L.; Neff, B.; Plane, J.; Platt, U.; Richter, A.; Roscoe, H.; Sander, R.; Shepson, P.; Sodeau, J.; Steffen, A.; Wagner, T.; Wolff, E. Halogens and their role in polar boundary-layer ozone depletion. *Atmos. Chem. Phys.* **2007**, *7*, 4375–4418.

12. Abbatt, J.P.D.; Thomas, J.L.; Abrahamsson, K.; Boxe, C.; Granfors, A.; Jones, A.E.; King, M.D.; Saiz-Lopez, A.; Shepson, P.B.; Sodeau, J.; Toohey, D.W.; Toubin, C.; von Glasow, R.; Wren, S.N.; Yang, X. Halogen activation via interactions with environmental ice and snow in the polar lower troposphere and other regions. *Atmos. Chem. Phys.* **2012**, *12*, 6237–6271.
13. Lehrer, E.; Hönninger, G.; Platt, U. A one dimensional model study of the mechanism of halogen liberation and vertical transport in the polar troposphere. *Atmos. Chem. Phys.* **2004**, *4*, 2427–2440.
14. Strong, C.; Fuentes, J.D.; Davis, R.E.; Bottenheim, J.W. Thermodynamic attributes of Arctic boundary layer ozone depletion. *Atmos. Environ.* **2002**, *36*, 2641–2652.
15. Morin, S.; Hönninger, G.; Staebler, R.M.; Bottenheim, J.W. A high time resolution study of boundary layer ozone chemistry and dynamics over the Arctic Ocean near Alert, Nunavut. *Geophys. Res. Lett.* **2005**, *32*, 165–176.
16. Jones, A.E.; Anderson, P.S.; Wolff, E.W.; Turner, J.; Rankin, A.M.; Colwell, S.R. A role for newly forming sea ice in springtime polar tropospheric ozone loss? Observational evidence from Halley station, Antarctica. *J. Geophys. Res. Atmos.* **2006**, *111*.
17. Cao, L.; Sihler, H.; Platt, U.; Gutheil, E. Numerical analysis of the chemical kinetic mechanisms of ozone depletion and halogen release in the polar troposphere. *Atmos. Chem. Phys.* **2014**, *14*, 3771–3787.
18. Evans, M.J.; Jacob, D.J.; Atlas, E.; Cantrell, C.A.; Eisele, F.; Flocke, F.; Fried, A.; Mauldin, R.L.; Ridley, B.A.; Wert, B.; Talbot, R.; Blake, D.; Heikes, B.; Snow, J.; Walega, J.; Weinheimer, A.J.; Dibb, J. Coupled evolution of BrO_x-ClO_x-HO_x-NO_x chemistry during bromine-catalyzed ozone depletion events in the Arctic boundary layer. *J. Geophys. Res. Atmos.* **2003**, *108*.
19. Piot, M.; Von Glasow, R. The potential importance of frost flowers, recycling on snow, and open leads for ozone depletion events. *Atmos. Chem. Phys.* **2008**, *8*, 2437–2467.
20. Piot, M.; Glasow, R. Modelling the multiphase near-surface chemistry related to ozone depletions in polar spring. *J. Atmos. Chem.* **2009**, *64*, 77–105.
21. Turanyi, T. KINAL - a program package for kinetic analysis of reaction mechanisms. *Comput. Chem.* **1990**, *14*, 253–254.
22. Cao, L.; Platt, U.; Gutheil, E. Role of the boundary layer in the occurrence and termination of the tropospheric ozone depletion events in polar spring. *Atmos. Environ.* **2016**, *132*, 98–110.
23. Atkins, P.; De Paula, J. *Elements of physical chemistry*; Oxford University Press, USA, 2013.
24. Atkinson, R.; Baulch, D.L.; Cox, R.A.; Crowley, J.N.; Hampson, R.F.; Hynes, R.G.; Jenkin, M.E.; Kerr, J.A.; Rossi, M.; Troe, J. Summary of Evaluated Kinetic and Photochemical Data for Atmospheric Chemistry. Technical report, 2006.
25. Stull, R.B. *An Introduction to Boundary Layer Meteorology*; Kluwer Academic Publishers: The Netherlands, 1988.
26. Jones, A.E.; Weller, R.; Wolff, E.W.; Jacobi, H.W. Speciation and rate of photochemical NO and NO_2 production in Antarctic snow. *Geophys. Res. Lett.* **2000**, *27*, 345–348.
27. Jones, A.E.; Weller, R.; Anderson, P.S.; Jacobi, H.W.; Wolff, E.W.; Schrems, O.; Miller, H. Measurements of NO_x emissions from the Antarctic snowpack. *Geophys. Res. Lett.* **2001**, *28*, 1499–1502.
28. Grannas, A.M.; Jones, A.E.; Dibb, J.; Ammann, M.; Anastasio, C.; Beine, H.J.; Bergin, M.; Bottenheim, J.; Boxe, C.S.; Carver, G.; Chen, G.; Crawford, J.H.; Dominé, F.; Frey, M.M.; Guzmán, M.I.; Heard, D.E.; Helmig, D.; Hoffmann, M.R.; Honrath, R.E.; Huey, L.G.; Hutterli, M.; Jacobi, H.W.; Klán, P.; Lefer, B.; McConnell, J.; Plane, J.; Sander, R.; Savarino, J.; Shepson, P.B.; Simpson, W.R.; Sodeau, J.R.; von Glasow, R.; Weller, R.; Wolff, E.W.; Zhu, T. An overview of snow photochemistry: evidence, mechanisms and impacts. *Atmos. Chem. Phys.* **2007**, *7*, 4329–4373.
29. Jacobi, H.W.; Frey, M.M.; Hutterli, M.A.; Bales, R.C.; Schrems, O.; Cullen, N.J.; Steffen, K.; Koehler, C. Measurements of hydrogen peroxide and formaldehyde exchange between the atmosphere and surface snow at Summit, Greenland. *Atmos. Environ.* **2002**, *36*, 2619 – 2628.
30. Gottwald, B.A.; Wanner, G. A reliable rosenbrock integrator for stiff differential equations. *Computing* **1981**, *26*, 355–360.
31. Valko, P.; Vajda, S. An extended ode solver for sensitivity calculations. *Comput. Chem.* **1984**, *8*, 255 – 271.
32. Turányi, T. Sensitivity analysis of complex kinetic systems. Tools and applications. *J. Math. Chem.* **1990**, *5*, 203–248.

33. Langendörfer, U.; Lehrer, E.; Wagenbach, D.; Platt, U. Observation of filterable bromine variabilities during arctic tropospheric ozone depletion events in high (1 hour) time resolution. *J. Atmos. Chem.* **1999**, *34*, 39–54.
34. Hausmann, M.; Platt, U. Spectroscopic measurement of bromine oxide and ozone in the high Arctic during Polar Sunrise Experiment 1992. *J. Geophys. Res. Atmos.* **1994**, *99*, 25399–25413.
35. Borken, J. Ozonabbau durch Halogene in der arktischen Grenzschicht. PhD thesis, Heidelberg University, 1996.
36. Barnes, I.; Becker, K.; Overath, R. Oxidation of organic sulfur compounds. In *The Tropospheric Chemistry of Ozone in the Polar Regions*; Niki, H.; Becker, K., Eds.; Springer Berlin Heidelberg, 1993; Vol. 7, pp. 371–383.
37. Aranda, A.; Le Bras, G.; La Verdet, G.; Poulet, G. The BrO + Ch_3O_2 reaction: Kinetics and role in the atmospheric ozone budget. *Geophys. Res. Lett.* **1997**, *24*, 2745–2748.
38. Sander, R.; Vogt, R.; Harris, G.W.; Crutzen, P.J. Modelling the chemistry of ozone, halogen compounds, and hydrocarbons in the arctic troposphere during spring. *Tellus B* **1997**, *49*, 522–532.
39. Mallard, W.G.; Westley, F.; Herron, J.T.; Hampson, R.F.; Frizzel, D.H. NIST chemical kinetics database: version 5.0. Technical report, Gaithersburg, 1993.
40. Fishman, J.; Carney, T.A. A one-dimensional photochemical model of the troposphere with planetary boundary-layer parameterization. *J. Atmos. Chem.* **1984**, *1*, 351–376.